Phosphorus Nitride P_3N_5: Synthesis, Spectroscopic, and Electron Microscopic Investigations

Wolfgang Schnick*

Laboratory for Inorganic Chemistry, University of Bayreuth, D-95440 Bayreuth, Germany

Jan Lücke

Institute of Materials Research, University of Bayreuth, D-95440 Bayreuth, Germany

Frank Krumeich

Institute for Inorganic Chemistry, University of Bonn, D-53117 Bonn, Germany

Received August 15, 1995. Revised Manuscript Received September 25, 1995⊗

Pure, stoichiometric, hydrogen-free, and crystalline phosphorus nitride P_3N_5 has been obtained for the first time by reaction of $(PNCl_2)_3$ and NH_4Cl between 770 and 1050 K. The compound has been characterized by elemental analyses, ^{31}P and ^{15}N MAS NMR, EXAFS, IR spectroscopy, X-ray powder diffraction, and electron microscopy. In the solid a three-dimensional cross-linked network structure of corner sharing PN_4 tetrahedra has been identified with $^2/_5$ of the nitrogen atoms bonded to three P atoms and $^3/_5$ of the nitrogen atoms bonded to two P atoms. By electron diffraction (ED) and high-resolution transmission electron microscopy (HRTEM) two distinguishable modifications α-P_3N_5 and β-P_3N_5 have been identified which differentiate only by the stacking order of identical sheets similar to the polytypes of SiC.

Introduction

In the past two decades, nonmetal nitrides have gained increasing interest. Particularly, the binary nitrides of boron and silicon (BN and Si_3N_4) have been used as high-performance materials because of their outstanding thermal, mechanical, and chemical stability.[1,2] Essential structural features for these specific properties are the strengths of the covalent bonds joining the constituent elements as well as the presence of highly cross-linked structures in the solid. For reasons of analogy, P_3N_5 should have a structure and properties, which resemble those of the above mentioned compounds BN and Si_3N_4. Nevertheless, reliable spectroscopic, crystallographic, and structural data of P_3N_5 have not as yet been reported in the literature, though the formation of binary phosphorus nitride during pyrolysis of polyphosphazenes has already been postulated.[3]

Recently, we have started a systematic investigation of binary and multinary nonmetal nitrides,[4] and we have mainly focused our interest on the phosphorus nitride class of compounds. The characteristic structural elements found in all phosphorus nitrides are PN_4 tetrahedra which may be linked via common vertexes showing differing degrees of condensation:[4] Isolated PN_4^{7-} anions are found in Li_7PN_4, whereas in $Li_{12}P_3N_9$ three PN_4 units form $P_3N_9^{12-}$ rings, analogously to cyclotrisilicates. Infinite chains of corner-sharing PN_4 tetrahedra occur in Ca_2PN_3. The smallest imaginable cage structure that can be formed from corner-sharing PN_4 tetrahedra has been found in $Li_{10}P_4N_{10}$, which contains the $P_4N_{10}^{10-}$ anion, the nitrido analogue of molecular phosphorus oxide P_4O_{10}. HPN_2, $LiPN_2$, and $Zn_7[P_{12}N_{24}]Cl_2$ each exhibit three-dimensional infinite network structures of corner-sharing PN_4 tetrahedra, which can be considered as the topological equivalent of β-cristobalite or of the sodalite framework, respectively.[4]

With a molar ratio of P:N = 3:5 phosphorus nitride (P_3N_5) has an intermediate composition with respect to SiO_2 (3:6) and Si_3N_4 (3:4). Accordingly, a cross-linked network structure of corner-sharing PN_4 tetrahedra might be expected for this binary nitride.[5]

Binary and ternary phosphorus nitrides have the potential for various ceramic applications, e.g., ionic conductors,[6] sintering additives,[7] pigments,[4] or microporous materials.[8]

In this paper we describe a new synthetic procedure which leads to pure, stoichiometric, hydrogen-free, and crystalline phosphorus nitride P_3N_5 for the first time. On pure samples of P_3N_5 we have obtained reliable

* To whom correspondence should be addressed.

⊗ Abstract published in *Advance ACS Abstracts,* November 1, 1995.

(1) Boberski, C.; Hamminger, R.; Peuckert, M.; Aldinger, F.; Dillinger, R.; Heinrich, J.; Huber, J. *Adv. Mater.* **1989**, *1*, 378.
(2) Paine, R. T.; Narula, C. K. *Chem. Rev.* **1990**, *90*, 73.
(3) Allcock, H. R.; Mc Donnell, G. S.; Riding, G. H.; Manners, I. *Chem. Mater.***1990**, *2*, 425.
(4) Schnick, W. *Angew. Chem., Int. Ed. Engl.* **1993**, *32*, 806.
(5) Veprek, S; Iqbal, Z.; Brunner, J.; Schärli, M. *Philos. Mag.* **1981,** *43*, 527.
(6) Schnick, W.; Lücke, J. *Solid State Ionics* **1990**, *38*, 271.
(7) Baldus, H. P.; Schnick, W.; Lücke, J.; Wannagat, U.; Bogedain, G., *Chem. Mater.* **1993**, *5*, 845.
(8) Schnick, W. *Stud. Surf. Sci. Catal.* **1994**, *84*, 2221.
(9) Baltkaula, A. A.; Miller, T. N.; Puzinja, I. A.; Ozolinsch, G. W.; Wajwad, A. Ja. *Latv. PSR Zinat. Akad. Vestis* **1968**, *6*, 761.
(10) Baltkaula, A. A.; Miller, T. N. *Latv. PSR Zinat. Akad. Vestis* **1971**, *4*, 389.
(11) Boden, G.; Sadowski, G.; Lehmann, H.-A. *Z. Chem.* **1971**, *11*, 114.
(12) Ronis, J. V.; Kuzjukevic, A. A.; Bondars, B. J.; Avotins, V. E.; Vitola, A. A.; *Latv. PSR Zinat. Akad. Vestis* **1986**, *3*, 366.

0897-4756/96/2808-0281$12.00/0

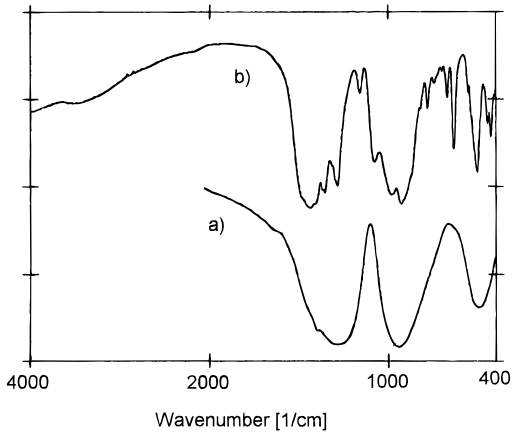

Figure 1. FT-IR spectra of phosphorus nitride (a) amorphous; (b) crystalline P_3N_5.

spectroscopic data. For the first time small single crystals of P_3N_5 have been grown and have been studied thoroughly, leading to an unambiguous crystallographic characterization of this important binary nitride which overcomes the contradictory results of former investigations.[9−12]

Experimental Section

Materials. Hexachlorocyclotriphosphazene (Merck Schuchardt) as well as ammonium chloride (Riedel-de-Haen) have been purified by sublimation in vacuum (330 K, $(PNCl_2)_3$; 450 K, NH_4Cl). $^{15}NH_4Cl$ was used for the synthesis of ^{15}N-enriched samples of P_3N_5.

All operations were carried out under purified argon atmosphere (O_2 < 0.5 ppm, H_2O < 0.1 ppm) using standard Schlenk technique or an inert gas glovebox (type MBRAUN 200).

Synthesis of P_3N_5. Stoichiometric amounts of $(PNCl_2)_3$ and NH_4Cl with molar ratio 1:2 are sealed in an evacuated thick-walled quartz ampule (length 150 mm, inner diameter 10 mm). The reaction mixture was held for 12 h at 770 K and for 24 h at 1050 K in an electrical tube furnace. To condense gaseous hydrogen chloride, which forms during the reaction, the ampules are cooled with liquid nitrogen and are opened under pure argon atmosphere. Surface deposits (NH_4Cl, $(PNCl_2)_3$, HCl) are removed by heating in vacuum (500 K). The product is obtained as a fine crystalline, colorless powder.

For elemental analyses the products were solubilized in a special digestion apparatus[13] at 460 K and 1.2 MPa (reaction time 2 days) in diluted sulfuric acid. During this reaction phosphorus nitride hydrolyzes forming ammonium hydrogen phosphate. Phosphorus and nitrogen were determined as molybdovanadato phosphate and indophenol blue, respectively. No deviations from the stoichiometric composition P_3N_5 have been detected. Even traces of silicon and chlorine have been detected neither in the solid (X-ray microprobe analysis) nor in the digested products. Equally, traces of oxygen have not been detected in the solid by WDX analyses (detection threshold ~0.5 mass %). The absence of hydrogen (N−H) has been proved by IR spectroscopy.

Physical Measurements. Infrared spectra were obtained on a Bruker IFS113v FTIR spectrometer equipped with a dry argon purge assembly and using a DTGS detector. Phosphorus nitride was ground in an agate mortar in the glovebox, mixed with potassium bromide (500 mg of KBr, dilution 1:1000) and pressed into pellets for transmission studies.

Solid-state NMR spectra were recorded on a Varian Unity 400 spectrometer (observing frequency 161.9 MHz (^{31}P) or 40.5 MHz (^{15}N)). Magic angle spinning (MAS) at 2−6 kHz was employed using cylindrical rotors made of boron nitride (diameter 5−7 mm, sample weight about 300 mg). Chemical

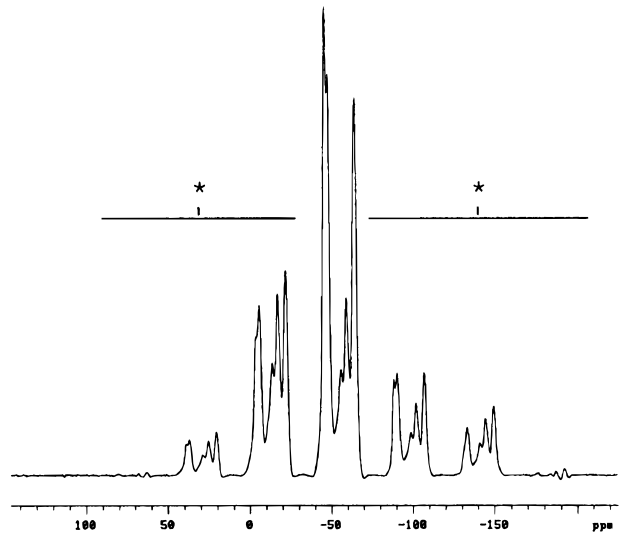

Figure 2. The 161.9-MHz ^{31}P solid state MAS NMR spectrum of P_3N_5 (* = rotational sidebands).

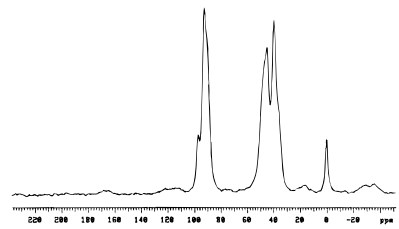

Figure 3. The 40.5-MHz ^{15}N solid state MAS NMR spectrum of P_3N_5.

shifts of phosphorus and nitrogen were referenced to H_3PO_4 (85%) and $^{15}NH_4Cl$, respectively. Because of the low natural occurrence of the ^{15}N isotope measurements on the nitrogen nucleus were performed on ^{15}N-enriched samples.

X-ray absorption experiments were performed at the ELSA high-energy storage ring (2.5 GeV, Physics Institute, University of Bonn). Powdered samples were homogeneously distributed on a capton foil and measured in transmission mode using double monochromators.

X-ray powder diffraction patterns were acquired using Cu $K\alpha_1$ radiation (λ = 154.056 pm) on a STOE STADI/P transmission powder diffractometer in Debye−Scherrer mode, equipped with a Ge-(111) single-crystal monochromator. Intensities were recorded by a position sensitive detector (mini-PSD, STOE) with an aperture of 2θ = 6.7°.

For electron microscopic investigations the microcrystalline samples were crushed in an agate mortar and dispersed in acetone. Some droplets of this dispersion were deposited on a copper grid covered with a perforated foil (carbon-coated Formvar). Selected area electron diffraction (SAED) investigations of microcrystals were performed using a 100 kV EM300 microscope (Philips) equipped with a goniometer stage which offers high tilting capability of ±60°. The use of a rotation holder allows to observe a crystal along different low-indexed zone axes. The evaluation of both several different electron diffraction patterns and the measured tilting angles between them enables a reconstruction of its reciprocal lattice (program TEMGIB[14]). The camera length of the microscope was calibrated using a polycrystalline Au standard. High-resolution transmission electron microscopy (HRTEM) was carried out on a EM400 microscope (Philips) working at 120 kV.

Results and Discussion

Synthesis and Properties of P_3N_5. Stoichiometric phosphorus nitride has been prepared according to eq 1 in 70% yield as a colorless powder.

(13) Buresch, O.; von Schnering, H. G., *Fresenius Z. Anal. Chem.* **1984**, *319*, 418.

(14) Czank, M.; Hogrefe, A. *Optik* **1991** (Supplement 4), *88*, 216.

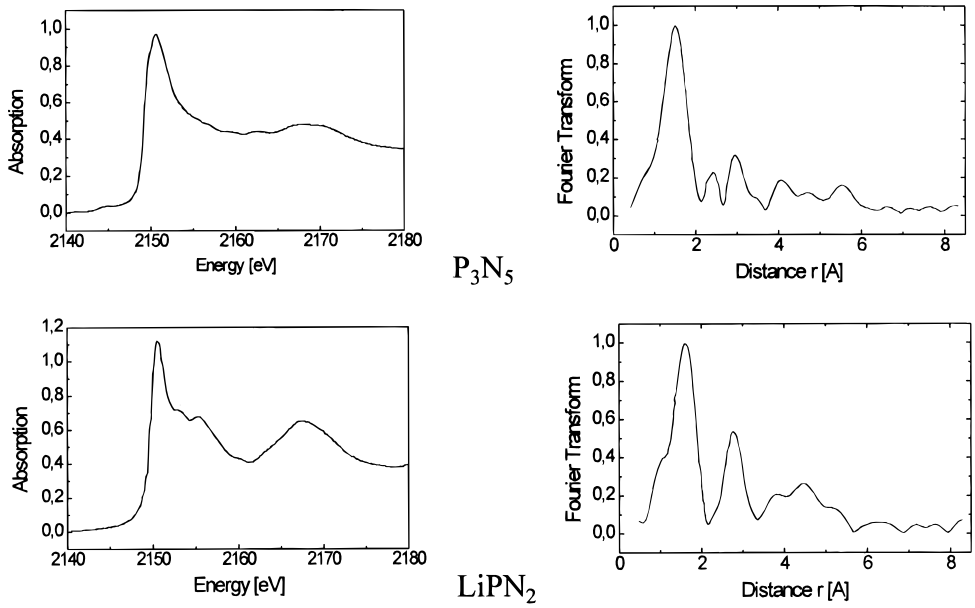

Figure 4. X-ray absorption spectra (left) of P_3N_5 and $LiPN_2$ and Fourier transforms (right).

$$(PNCl_2)_3 + 2NH_4Cl \rightarrow P_3N_5 + 8HCl \qquad (1)$$

Matching a molar ratio of P:N = 3:5 in the starting mixtures is essential in order to obtain this ratio in the solid, too. Otherwise, the yield decreases and other phases ($H_{3x}P_3N_{5+x}$, $0 < x < 1$) are obtained. At lower temperatures (<1000 K) amorphous samples were obtained whereas at higher temperatures (>1100 K) decomposition of the desired product led to nonstoichiometric materials. Phosphorus nitride is nonsensitive to air or moisture, insoluble in acids and bases as well as in organic solvents under normal pressure. Thermal degradation starts at temperatures above 1100 K yielding gaseous species like N_2, PN, and P_4.

Spectroscopic Investigations. No hydrogen bonds (N−H or P−H) are left in the solid as can be seen in the infrared spectra (Figure 1). Two broad absorption bands at about 950 and 1350 cm^{-1}, which split off in the crystalline samples, are detected. They are originated from P−N stretching modes[15] as confirmed by the comparison of ^{14}N− and $^{15}N-P_3N_5$ spectra.

NMR investigations on the phosphorus nucleus ^{31}P (Figure 2) show several well-resolved signals between −40 and −70 ppm surrounded by side bands at a distance of 6080 Hz (=rotation frequency). Five signals were detected at −46.0, −48.2, −56.2, -59.7, and −64.8 ppm with an intensity ratio of about 5:5:1:1:4, respectively. In the ^{15}N solid-state NMR experiments (Figure 3) two groups of signals at 40 and 90 ppm appear beside the signal at 0 ppm which is attributed to $^{15}NH_4Cl$ used as an internal standard.

Figure 4 shows the X-ray absorption spectra (left side) and the resulting Fourier transforms (right side) of P_3N_5 and $LiPN_2$. The onset of the absorption at about 2140 eV (maximum at 2151 eV) as well as the maxima in the Fourier transforms (at about 165 and 290 pm) are very similar in both phosphorus nitrides. Referring to the well-known structure of $LiPN_2$,[16] the maximum in the absorption spectrum of P_3N_5 is derived from phosphorus atoms in their highest possible oxidation state P^V, those in the Fourier transform are associated with P−N− bonds (167 pm) and P···P distances (295 pm), respectively. Furthermore, the IR investigation as well as the EXAFS results indicate that stoichiometric phosphorus nitride P_3N_5 consists of a threedimensional network of PN_4 tetrahedra connected by common vertexes. No other than P^{+V} N^{-III} bonds were detected (IR, EXAFS) which has qualitatively been postulated by Veprek.[5] The mean bond length is about 167(5) pm which is in good agreement with theoretical calculations based on bond-valence parameters.[17] From the P···P-distance (295 ppm) a P−N−P-bonding angle of 124° is calculated which is comparable to those found in other ternary phosphorus nitrides.[4] There are at least five distinguishable, magnetic different phosphorus atoms (^{31}P MAS NMR) with a chemical shift at higher field (about −50 ppm) compared to non-cross-linked compounds with tetrahedrally coordinated phosphorus, e.g., $P(NH_2)_4I$: σ = 14.2 ppm.[18,19] Investigations on the ^{15}N nucleus show two signal groups with a ratio of 3:2. In contrast to the oxygen atom (maximum coordination number in silicates and phosphates: CN = 2) nitrogen atoms may form one, two, or three covalent bonds to phosphorus. Thus, according to the results of Bunker et al.,[20] the signals at 40 and 90 ppm were assigned to nitrogen atoms which are bonded to two ($N^{[2]}$) or three phosphorus atoms ($N^{[3]}$), respectively. The ratio of 3:2 estimated by quantitative analysis of the NMR spectrum is in good agreement with theoretical considerations (Table 1). The

Table 1. Ratio of 2-fold ($N^{[2]}$) to 3-fold ($N^{[3]}$) Bonded Nitrogen Atoms in Phosphorus Nitrides

	compound	$NH^{[2]}:N^{[2]}:N^{[3]}$
general	$H_{3x}P_3N_{5+x}$	$3x:3:(2-2x)$
$x = 0$	P_3N_5	0:3:2
$x = 1$	HPN_2	1:1:0

(15) Schnick, W.; Lücke, J. *Z. Anorg. Allg. Chem.* **1992**, *610*, 121.
(16) Schnick, W.; Lücke, J. *Z. Anorg. Allg. Chem.* **1990**, *588*, 19.
(17) Brese, N. E.; O'Keeffe, M. *Acta Crystallogr.* **1991**, *B47*, 192.
(18) Schnick, W.; Horstmann, S.; Schmidpeter, A. *Angew. Chem., Int. Ed. Engl.* ***1994***, *33*, 785.
(19) Horstmann, S.; Schnick, W., *Z. Naturforsch.* **1994**, *B50*, 1381.
(20) Bunker, B. C.; Tallant, D. R.; Balfe, C. A.; Kirkpatrick, R. J.; Turner, G. L.; Reidmeyer, M. R. *J. Am. Ceram. Soc.* **1987**, *70*, 675.
(21) Grün, R. *Acta Crystallogr.* **1979,** *B35*, 800.
(22) Krumeich, F.; Lücke, J.; Schnick, W. *Electron Microsc.* **1992**, *2*, 423.

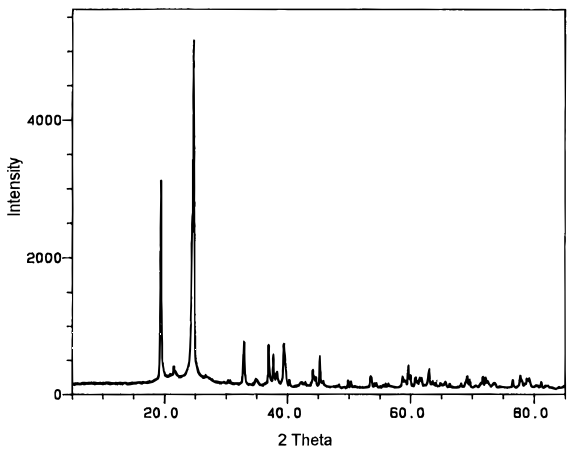

Figure 5. X-ray powder diffraction pattern of P_3N_5.

Table 2. Structure Units in Polymeric Nitrides

compound	$N^{[2]}$	$N^{[3]}$
HPN_2[15]	only	
P_3N_5	3	2
$SiPN_3$[7]	1	2
Si_3N_4[21]		only

two different types of nitrogen atoms in P_3N_5 ($N^{[2]}$ and $N^{[3]}$) require different P−N bond lengths. However, a resolution of this difference by the EXAFS method has not been achieved.

The amount of 3-fold-bonded nitrogen rises from HPN_2 (no $N^{[3]}$)[15] to P_3N_5 ($N^{[2]}$:$N^{[3]}$ = 3:2), $SiPN_3$ (1:2),[7] and Si_3N_4 (only $N^{[3]}$),[21] as summarized in Table 2.

Determination of Lattice Parameters. The as-received samples contain only small crystallites (REM <5 μm). The X-ray powder diffraction pattern (Figure 5) shows only two strong reflections (2θ = 19.5 and 24.7°) beside several broad ones above 2θ = 30°. All indexing trials fail due to the low number of resolvable reflections, which could not be increased at higher resolution in the synchrotron experiment.

Nevertheless we succeeded in finding microscopic single crystals suitable for electron microscopy.[22] Their thorough examination led to the discovery of two different modifications which we refer to as α- and β-P_3N_5.

Table 3. Observed and Calculated Tilting Angles between Reciprocal Lattice Planes in α-P_3N_5

zone axis	ϕ	$\Delta\phi$(exp)	$\Delta\phi$(calc)
$[10\bar{1}]^*$	−61		
$[2\bar{1}\bar{1}]^*$	−48	13	15.6
$[1\bar{1}0]^*$	−32	16	16.5
$[2\bar{3}1]^*$	−16	16	14.8
$[1\bar{2}1]^*$	−5	11	11.9
$[1\bar{3}2]^*$	+11	16	15.7
$[1\bar{4}3]^*$	+20	9	9.1
$[1\bar{5}4]^*$	+26	6	6.5
$[0\bar{1}1]^*$	+47	21	21.6

Both were characterized concerning their lattice parameters and symmetry using the electron diffraction method.

The lattice parameters of α-P_3N_5 were obtained by analyzing the electron diffraction patterns of a crystal tilted around the [111]* axis:

$$a = 1650(10), \quad b = 580(5), \quad c = 810(6)\ \text{pm}$$
$$\alpha = \beta = \gamma = 90°$$

The observed tilting angles are in good agreement with the calculated ones (Table 3).

Considering the observed systematic extinctions (hkl: $h + k$, $h + l$, and $k + l$ odd) we conclude that α-P_3N_5 has a face-centered orthorhombic unit cell. Furthermore, the electron diffraction pattern along [010]* (Figure 6) shows reflections only with h and l even ($h + l = 4n$ for $h0l$) indicating a diamond glide plane. These observations lead to the possible space groups $Fdd2$ (no. 43) and $Fddd$ (no. 70).

Crystallites of the β-phase were easily recognizable by superstructure reflections indicating a unit cell larger (factor 1.5) than that found for α-P_3N_5. A series of diffraction patterns obtained by tilting a crystal around [001]* (Figure 7) enabled the determination of the lattice parameters:

$$a = 913(8), \quad b = 585(5), \quad c = 2170(15)\ \text{pm}$$
$$\alpha = \beta = \gamma = 90°$$

A 6-fold superstructure is clearly visible along [010]* and other directions $[uvw]^*$ with $v \neq 0$ whereas in the

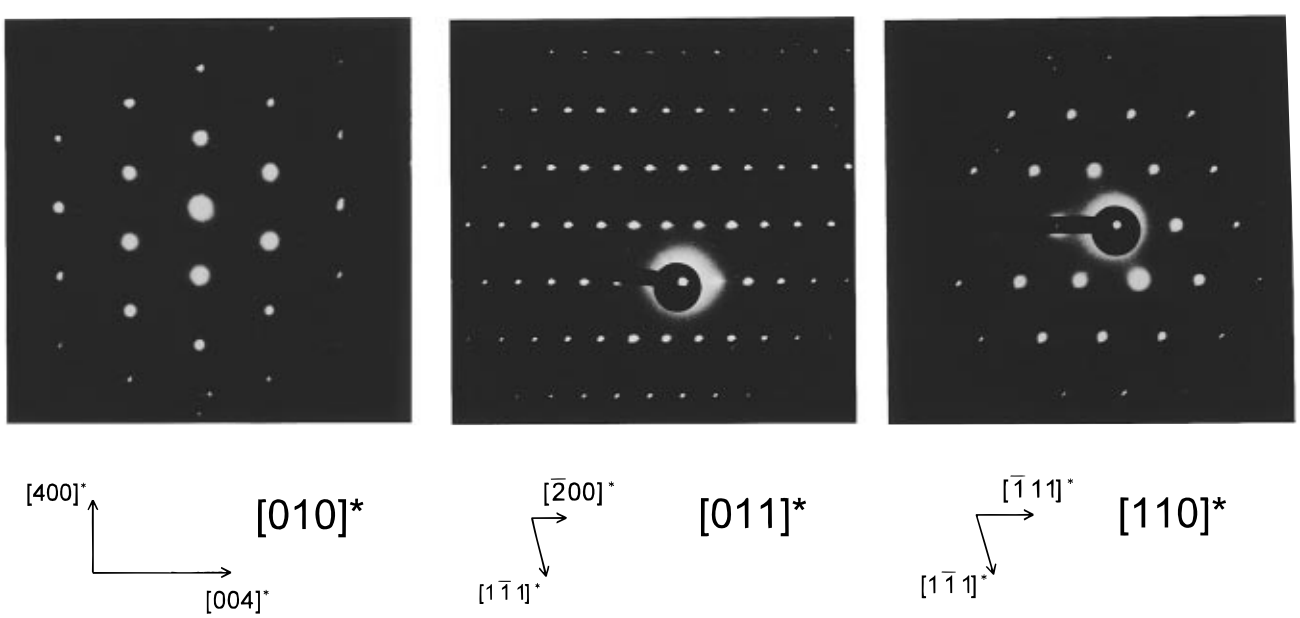

Figure 6. SAED of α-P_3N_5 along [010]*/[011]*/[110]* (from left to right).

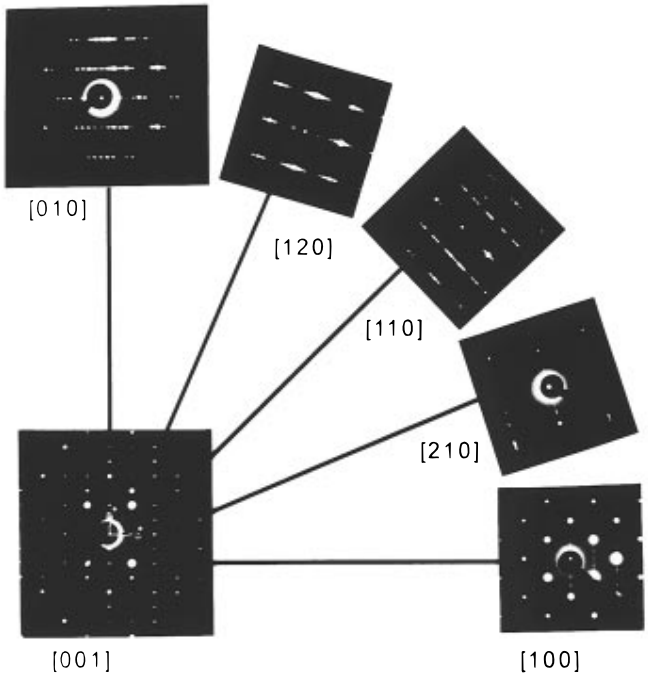

Figure 7. Tilting series of β-P_3N_5.

*bc** plane only two weak and diffuse spots lay between the main reflections; furthermore, diffuse streaking is observed along [001]* indicating an amount of disorder. Moreover, reflection conditions are observed in the [100]* ($k + l = 2n$ for $0kl$) and [010]* diffraction pattern ($h = 2n$ for $h0l$). These extinctions point out an axial and a diagonal glide plane for β-P_3N_5. Further extinctions may occur in the *ab** plane but have not been observed because of multiple scattering producing forbidden reflections. Thus, the lattice parameters reported in the literature[9−12] are very contrary to our results and might have been determined on either impure samples regarding the oxygen and hydrogen content or resulted from multiphase powder diffraction data which lead to incorrect parameters.

Relation between α- and β-P_3N_5. By comparison of the two unit cells of both modifications, the remarkable coincidence of the β axes is conspicuous. A metrical relationship between the two cells may be approximated by

$$\begin{bmatrix} a \\ b \\ c \end{bmatrix}_{\beta-P_3N_5} = \begin{bmatrix} 1/2 & 0 & 1/2 \\ 0 & 1 & 0 \\ 3/4 & 0 & -9/4 \end{bmatrix} \times \begin{bmatrix} a \\ b \\ c \end{bmatrix}_{\alpha-P_3N_5}$$

In particular, this relationship becomes obvious by examination of the $[1\bar{2}1]^*$ (α-P_3N_5) and $[110]^*$ (β-P_3N_5) zone axes, respectively. The strong reflections of the β phase are located at the same sites in the corresponding electron diffraction pattern as the spots of α-P_3N_5 (Figure 8a). Additionally, in β-P_3N_5 five weaker spots between the strong reflection are observed. The HR-TEM images illustrate the relationship: Using imaging conditions near Scherzer defocus, both phases exhibit lines of bright dots along $[10\bar{1}]^*$ (α-P_3N_5) and $[110]^*$ (β-P_3N_5), respectively; the distance between the dots is equal in $[531]^*\alpha$ and $[110]^*\beta$ direction (Figure 8b). Actually, in both phases these lines turned out to be stacked identical sheets (parallel to the *ab* plane of β-P_3N_5). In α-P_3N_5 an infinite sequence of the dots in $[10\bar{1}]^*\alpha$ direction results, whereas in the β form each three sheets the direction of stacking turns resulting in a zigzag chain of bright dots which gives rise to the 6-fold superstructure along *c* (Figure 8b). The seventh bright dot represents the translation period along the *c* axis. In α-P_3N_5 there is no translation perpendicular to [531]* because of an angle of 87.9° between [531]* and [101]*.

Several crystallites show both kinds of stacking in adjacent areas (Figure 8c). This fact, as well as the difficulty to yield larger amounts of the phases separately, indicates a small difference of energy between both modifications. Furthermore the 6-fold superstructure is scarcely observed in pure form; most crystals exhibit heavy stacking disorder as indicated by disturbed superstructure reflections and diffuse scattering along *c**. The nature of this features becomes obvious from highly resolved TEM images, where several different stacking periods are recognizable (Figure 8c).

Conclusions

Crystalline P_3N_5 is built up by a three-dimensional network structure of corner sharing PN_4 tetrahedra

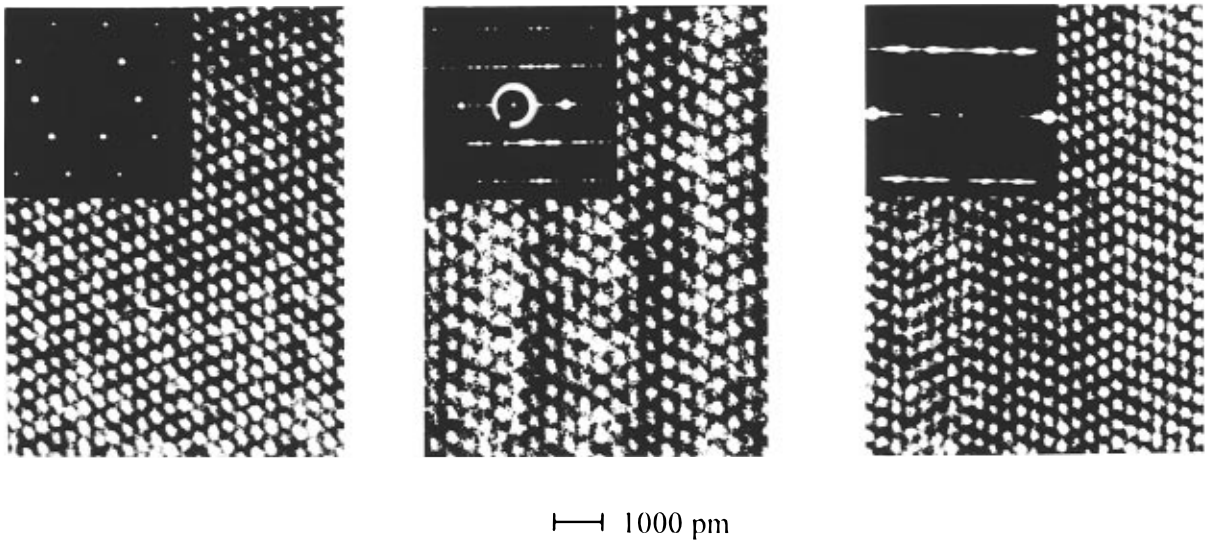

Figure 8. High-resolution images with SAED insets (a) along $[1\bar{2}1]_\alpha$ (left), (b) along $[110]_\beta$ (middle), and (c) stacking disorder in P_3N_5 (right).

according to ${}^{3}_{\infty}[P_3^{[4]}N_3^{[2]}N_2^{[3]}]$ (I).

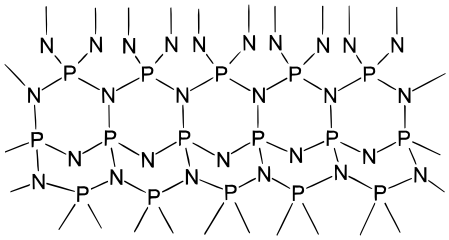

Only the combination of spectroscopical and diffraction methods, especially electron microscopy for structural analysis, enables a detailed structural and crystallographic characterization of P_3N_5 as no conventional single-crystal data for structure determination have been available for this compound.

A representative for an unique binary structure type was found for the first time which combines a tetrahedral structure with the very rare molar ratio of 3:5 for the constituent elements.

Little energetic differences in the stacking variations of P_3N_5 lead to a structural diversity resulting in the formation of polytypes that remind us of those found in polytypes of SiC.

Consequently, the growth of macroscopic ordered single crystals of P_3N_5 polytypes has to be performed in order to determine the unique structure of this important binary nitride that is currently in progress.

Acknowledgment. The preparative part of this work has been performed at the Institute for Inorganic Chemistry, Bonn University. The authors would like to thank Prof. Dr. M. Jansen for support and Prof. J. Hormes, Physics Institute, Bonn University, for EXAFS measurements. Financial support by the Ministerium für Wissenschaft und Forschung des Landes Nordrhein-Westfalen, the Deutsche Forschungsgemeinschaft (project Schn377/2-1 and Heisenberg grant for W.S.), as well as the Fonds der Chemischen Ind. is greatfully acknowledged. Helpful discussions and support during the preparation of the manuscript by Stefan Horstmann, University of Bayreuth, is gratefully acknowledged.

CM950385Y